iScience

CellPress
OPEN ACCESS

Article

Transcriptomic characterization of lung pericytes in systemic sclerosis-associated pulmonary fibrosis

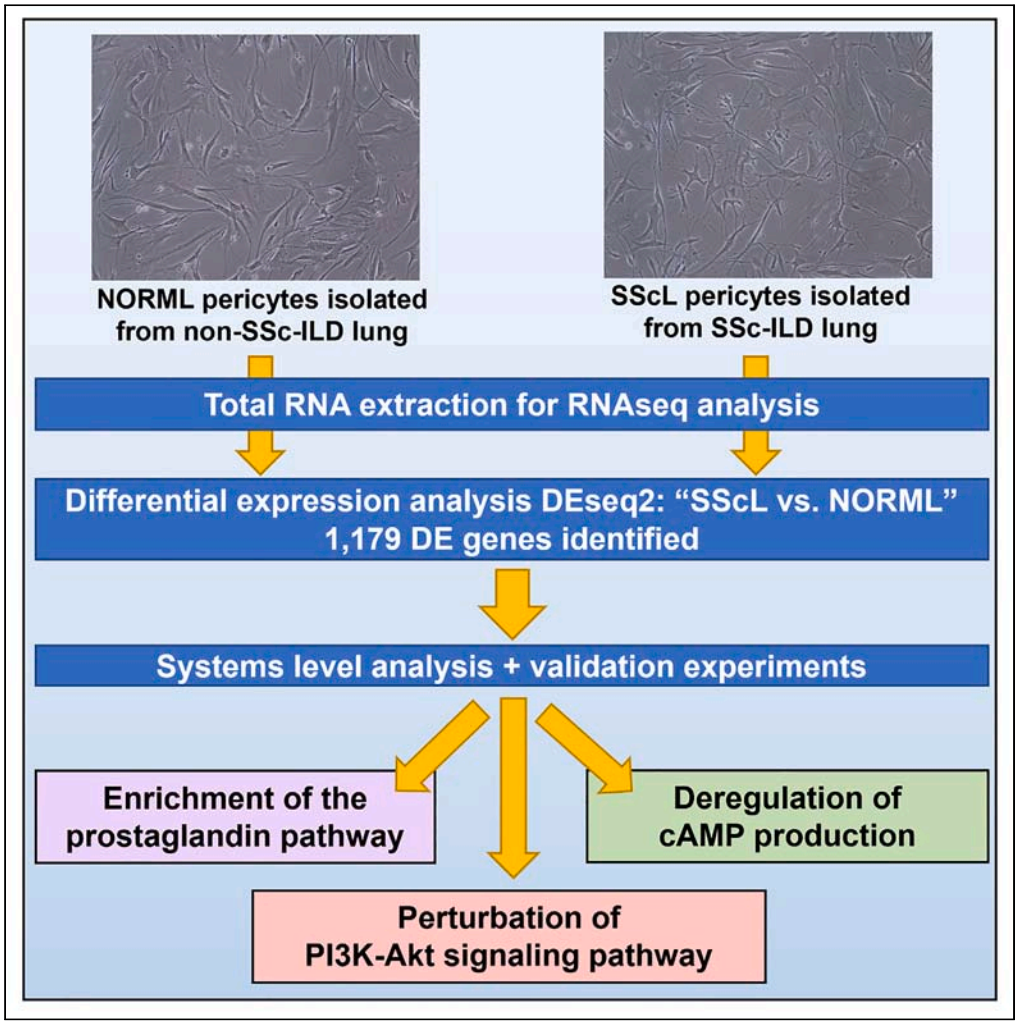

Ludivine Renaud, Carole L. Wilson, Robert Lafyatis, Lynn M. Schnapp, Carol A. Feghali-Bostwick

feghalib@musc.edu

Highlights

1,179 differentially expressed genes were observed in the pericytes of SSc lungs

Prostaglandin, PI3K-AKT, calcium, and vascular remodeling pathways were impacted

This enrichment contributed to lung fibrosis and vascular dysfunction in SSc lungs

This signature suggests loss of protection against inflammation and fibrosis

Renaud et al., iScience 27, 110010
June 21, 2024
https://doi.org/10.1016/j.isci.2024.110010

iScience

CellPress
OPEN ACCESS

Article

Transcriptomic characterization of lung pericytes in systemic sclerosis-associated pulmonary fibrosis

Ludivine Renaud,[1,4] Carole L. Wilson,[1,2,4] Robert Lafyatis,[3] Lynn M. Schnapp,[1,2,5] and Carol A. Feghali-Bostwick[1,5,6,*]

SUMMARY

Systemic sclerosis (SSc) is a chronic disease characterized by fibrosis and vascular abnormalities in the skin and internal organs, including the lung. SSc-associated pulmonary fibrosis (SSc-PF) is the leading cause of death in SSc patients. Pericytes are key regulators of vascular integrity and endothelial function. The role that pericytes play in SSc-PF remains unclear. We compared the transcriptome of pericytes from SSc-PF lungs (SScL) to pericytes from normal lungs (NORML). We identified 1,179 differentially expressed genes in SScL pericytes. Pathways enriched in SScL pericytes included prostaglandin, PI3K-AKT, calcium, and vascular remodeling signaling. Decreased cyclic AMP production and altered phosphorylation of AKT in response to prostaglandin E2 in SScL pericytes demonstrate the functional consequence of changes in the prostaglandin pathway that may contribute to fibrosis. The transcriptomic signature of SSc lung pericytes suggests that they promote vascular dysfunction and contribute to the loss of protection against lung inflammation and fibrosis.

INTRODUCTION

Systemic sclerosis (SSc) is an autoimmune disorder characterized by fibrosis of the skin and internal organs and vasculopathy.[1,2] Pulmonary involvement is common in SSc, and SSc-associated pulmonary fibrosis (SSc-PF) is the leading cause of death in SSc patients.[3] Pericytes are perivascular cells of mesenchymal origin that are embedded within the basement membrane of microvessels,[4] where they play a critical role in maintaining the integrity of the vasculature. Pericytes are most often characterized by the expression of platelet-derived growth factor receptor β (*PDGFRB*). Several studies showed alterations in pericyte phenotype and density in sclerotic skin.[5,6] A recent study by Valenzi et al. showed expansion of pericytes in SSc-PF lungs.[7]

Hallmark traits of SSc include micro-angiopathy, characterized by a decrease in capillary density, disorganized architecture, and impaired reparative angiogenesis, overall leading to reduced blood flow and tissue hypoxia, i.e., fingertip ulcers.[8,9] Additionally, the excessive buildup of extracellular matrix (ECM) components increases the spread of the blood vessel network, contributing even more to tissue hypoxia.[8] Pericytes play an important role in normal angiogenesis and vascular homeostasis, due to their ability to crosstalk with endothelial cells via the release of growth factors, direct cell-cell interaction, and modulation of the ECM.[10] Vascular endothelial growth factor (VEGF) signaling and the expression of VEGF receptors are key regulators of angiogenesis, and both endothelial cells and pericytes can promote angiogenesis via the VEGF-VEGFR2 axis.[11] Pericytes also express *VEGFR1*, a decoy of VEGFR2 able to bind endogenous VEGF, and by doing so pericytes can negatively regulate VEGFR2-driven angiogenesis.[12] The TIE2 receptor, encoded by the gene *TEK*, is another pericyte-expressed receptor that plays a role in angiogenesis as its deletion promotes angiogenesis.[13]

The contribution of pericytes to SSc is incompletely understood. We and others have demonstrated that pericytes may contribute to fibrosis by transdifferentiation into myofibroblasts,[14–17] the key effector cell in fibrosis, including in a study in SSc skin.[18,19] Additionally, pericytes have the ability to differentiate into different lineages and are often considered as mesenchymal stem cells of crucial importance in SSc.[20] Interestingly, SSc pericytes, fibroblasts, and myofibroblasts all express A disintegrin and metalloproteinase domain 12 (*ADAM12*), alpha smooth muscle actin (*αSMA*), the extra domain A (*EDA*) variant of fibronectin, and Thy-1 cell surface antigen (*THY1*).[21] Our goal is to provide insights into the molecular signature and potential role of pericytes in SSc-PF.

[1]Department of Medicine, Medical University of South Carolina, Charleston, SC 29425, USA
[2]Department of Medicine, University of Wisconsin, Madison, WI 53705, USA
[3]Department of Medicine, University of Pittsburgh Medical Center, Pittsburgh, PA 15213, USA
[4]These authors contributed equally
[5]Senior author
[6]Lead contact
*Correspondence: feghalib@musc.edu
https://doi.org/10.1016/j.isci.2024.110010

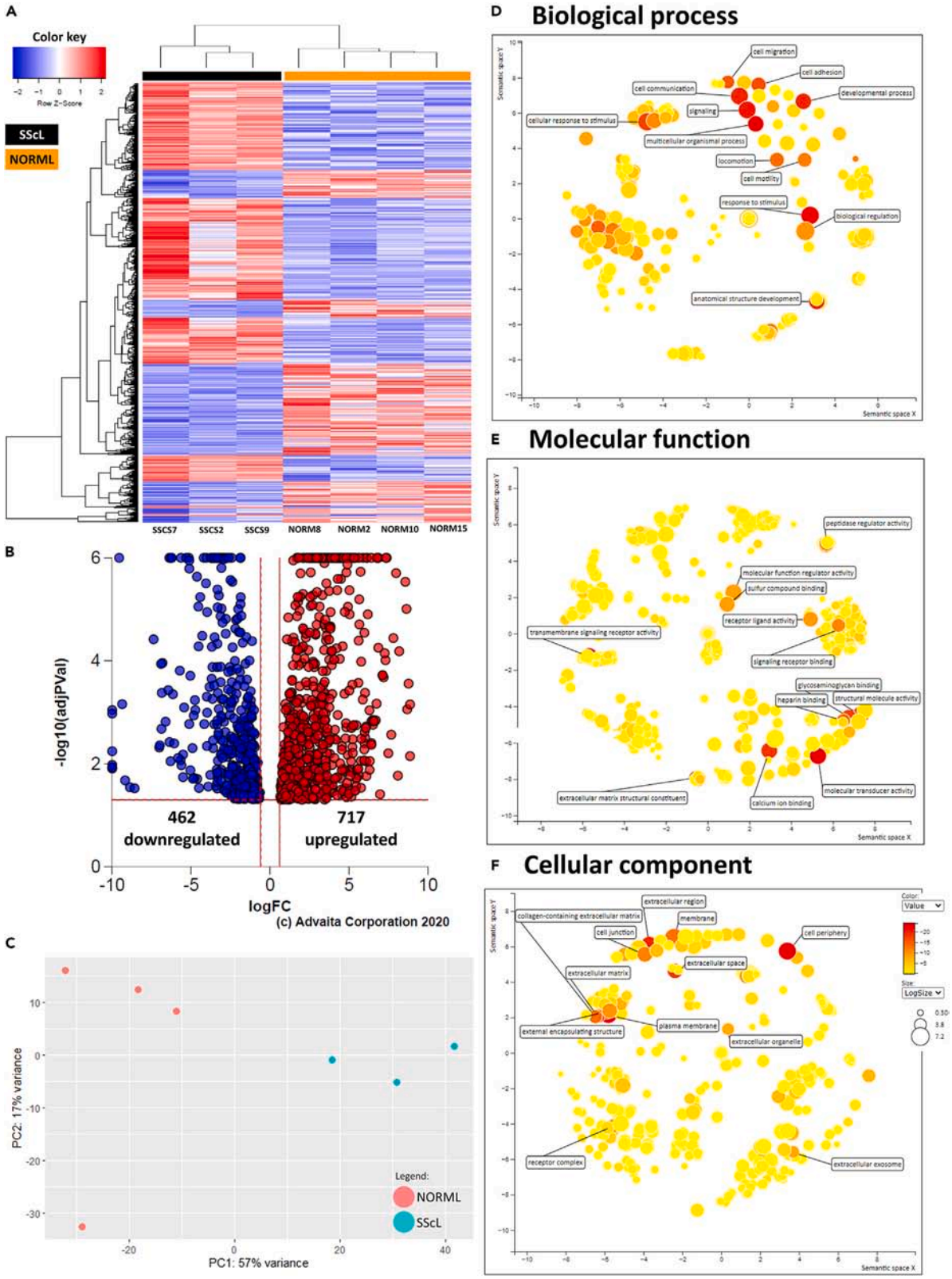
A
Color key
Row Z-Score
SScL
NORML
SSCS7
SSCS2
SSCS9
NORM8
NORM2
NORM10
NORM15
B
-log10(adjPVal)
462
downregulated
717
upregulated
logFC
(c) Advaita Corporation 2020
C
PC2: 17% variance
PC1: 57% variance
Legend:
NORML
SScL
D
Biological process
cell migration
cell adhesion
cell communication
developmental process
signaling
cellular response to stimulus
multicellular organismal process
locomotion
cell motility
response to stimulus
biological regulation
anatomical structure development
Semantic space X
Semantic space Y
E
Molecular function
peptidase regulator activity
molecular function regulator activity
sulfur compound binding
receptor ligand activity
transmembrane signaling receptor activity
signaling receptor binding
glycosaminoglycan binding
heparin binding
structural molecule activity
extracellular matrix structural constituent
calcium ion binding
molecular transducer activity
F
Cellular component
extracellular region
collagen-containing extracellular matrix
membrane
cell junction
cell periphery
extracellular space
extracellular matrix
external encapsulating structure
plasma membrane
extracellular organelle
receptor complex
extracellular exosome
Color:
Value
Size:
LogSize

Figure 1. Differential expression analysis of "SScL vs. NORML" pericytes

(A) Heatmap for all the genes with a padj value <0.05.

(B) Volcano plot showing all the DE genes that are up- and downregulated according to the following criteria of significance: padj <0.05, which is equal to 1.3 in the -log10 scale shown on the y axis, and log2FC of at least 0.6 (shown on x axis as logFC in Advaita generated volcano plot).

(C) PCA plot showing the distribution and clustering of the SScL and NORML samples.

(D–F) For each category of GO terms, the iPathwayGuide-generated *p* values and their respective GO-ID were entered in REViGO to obtain scatterplots showing the cluster representatives (i.e., terms remaining after the redundancy reduction) in a two-dimensional space derived by applying multidimensional scaling to a matrix of the GO terms' semantic similarities. Bubble color indicates the user-provided *p* value and terms in red are more significant than the ones in yellow (legend in (F), top-right corner); size indicates the frequency of the GO term in the underlying GOA database (bubbles of more general terms are larger). The top 12 most enriched GO terms are labeled in each scatterplot.

To identify signatures that are different in SSc and control pericytes, bulk RNA sequencing (RNA-seq) was performed on total RNA extracted from primary human pericytes outgrown from the lungs of (1) patients with severe SSc-PF (abbreviated as SScL) and (2) organ donors whose non-fibrotic lungs were not used for transplantation (hereafter referred to as "normal" and abbreviated as NORML). Differential expression (DE) genes were identified by DEseq2 differential expression analysis "SScL vs. NORML" to characterize the transcriptomic signature of SSc lung pericytes. Impacted pathways and functional enrichment were defined by systems level analysis.

RESULTS

Isolation and characterization of SSc and normal lung pericytes

To define the transcriptomics profile of pericytes from SSc (designated "SScL") and non-fibrotic ("normal," designated "NORML") lungs, we performed bulk RNA-seq analysis of pericytes cultured *in vitro*. This approach is particularly desirable for mesenchymal cells, which often show a tissue dissociation bias in typical single-cell RNA-seq (scRNA-seq) analyses.[22] Lung tissue specimens were obtained from SSc patients with severe disease undergoing transplantation; for normal controls, tissue was collected from donors whose lungs were not used for transplantation but were without fibrosis or a known lung disease (Table S1). The tissue was minced and enzymatically digested, and the resulting cells were cultured in a specialized medium that pre-selects for pericytes, as we and others have shown previously.[17,23,24] To further enrich for pericytes, we performed magnetic bead selection of the cultured cells for PDGFRβ positivity.

Differential expression analysis of SSc vs. normal lung pericytes

The differential expression analysis "SScL vs. NORML" yielded 1,179 DE genes (*padj* < 0.05, log2FC at least |0.6|, Table S2), of which 717 were upregulated and 462 were downregulated in SSc lung pericytes compared to normal (Figures 1A and 1B). The SScL and NORML samples clustered well as shown by the heatmap and the principal-component analysis (PCA) plot (Figures 1A–1C). Using iPathwayGuide, we determined that 1,925 gene ontology (GO) terms were enriched in SSc lung pericytes (Figures 1D–1F; Table S3). Some of the most impacted Biological Process terms were related to developmental process, response to stimulus and signaling (Figure 1D). Under the Molecular Function category, some of the most enriched terms pertained to the molecular transducer activity, calcium ion binding and ECM structural constituent (Figure 1E). In the Cellular Component category, terms pertaining to plasma membrane, extracellular region, and cell periphery, among others, were highly deregulated (Figure 1F). iPathwayGuide analysis also showed that 39 pathways were enriched in SSc lung pericytes (*p* value <0.05) (Figure 2; Table S4).

We compared the list of DE genes identified in cultured pericytes to the DE genes identified previously in pericytes using scRNA-seq analysis of lung tissues of SSc-PF patients.[7] We identified 41 DE genes that are overlapping between our study and the one done by Valenzi et al. (Figure S1).

Hub genes analysis: GNG4

We used iPathwayGuide to identify hub genes with high centrality degree (CD). Table 1 shows all hub genes with a CD ≥ 0.20. The hub gene at the center of this network and with the highest centrality degree (CD = 1.00) is G-protein subunit gamma 4 (GNG4) (Figure 3A). Our RNA-seq data revealed that GNG4 is significantly upregulated in SSc lung pericytes (*padj* = 1.61E-03, log2FC = 2.92) and is directly connected to 19 DE genes: *RAMP2*, *GIPR*, *EDNRA*, *EDNRB*, *FPR1*, *C3AR1*, *C3*, *CCR1*, *CCL13*, *CX3CL1*, *PTGER3*, *ADRA1D*, *APLN*, *PTGDR2*, *GPR4*, *GPR143*, *CCK*, *GNAZ*, and *KCNJ15*. Note that some of these are also hub genes (denoted by the asterisks in Table 1). We also confirmed by quantitative PCR analysis (qPCR) that *GNG4* is highly expressed in the majority of SSc lung pericytes as compared to normal (Figure 3B).

Perturbation of the prostaglandin signaling pathway in SSc lung pericytes

We identified prostaglandin E receptor 3 (*PTGER3*) as another hub gene that is connected to *GNG4* and is upregulated in SSc lung pericytes (Figure 3A; Table 1). Concomitantly, prostaglandin E receptor 2 (*PTGER2*), prostaglandin D2 receptor 2 (*PTGDR2*), and prostaglandin-endoperoxide synthase 1 (*PTGS1*) are downregulated in these cells (Tables 1 and S2). qPCR analysis confirmed that *PTGER2* is significantly downregulated in SSc lung pericytes, with a trend toward upregulation of *PTGER3* in SScL pericytes relative to normal pericytes (Figures 4A and 4B).

To determine functional significance of prostaglandin receptor changes, we measured cAMP levels in SScL and NORML pericytes treated with PGE2, forskolin (a receptor-independent stimulator of cAMP production), or vehicle (Figure 4C). Levels of cAMP increased in normal lung pericytes treated with either PGE2 or forskolin as compared to vehicle control. However, SScL pericytes responded less robustly than NORML

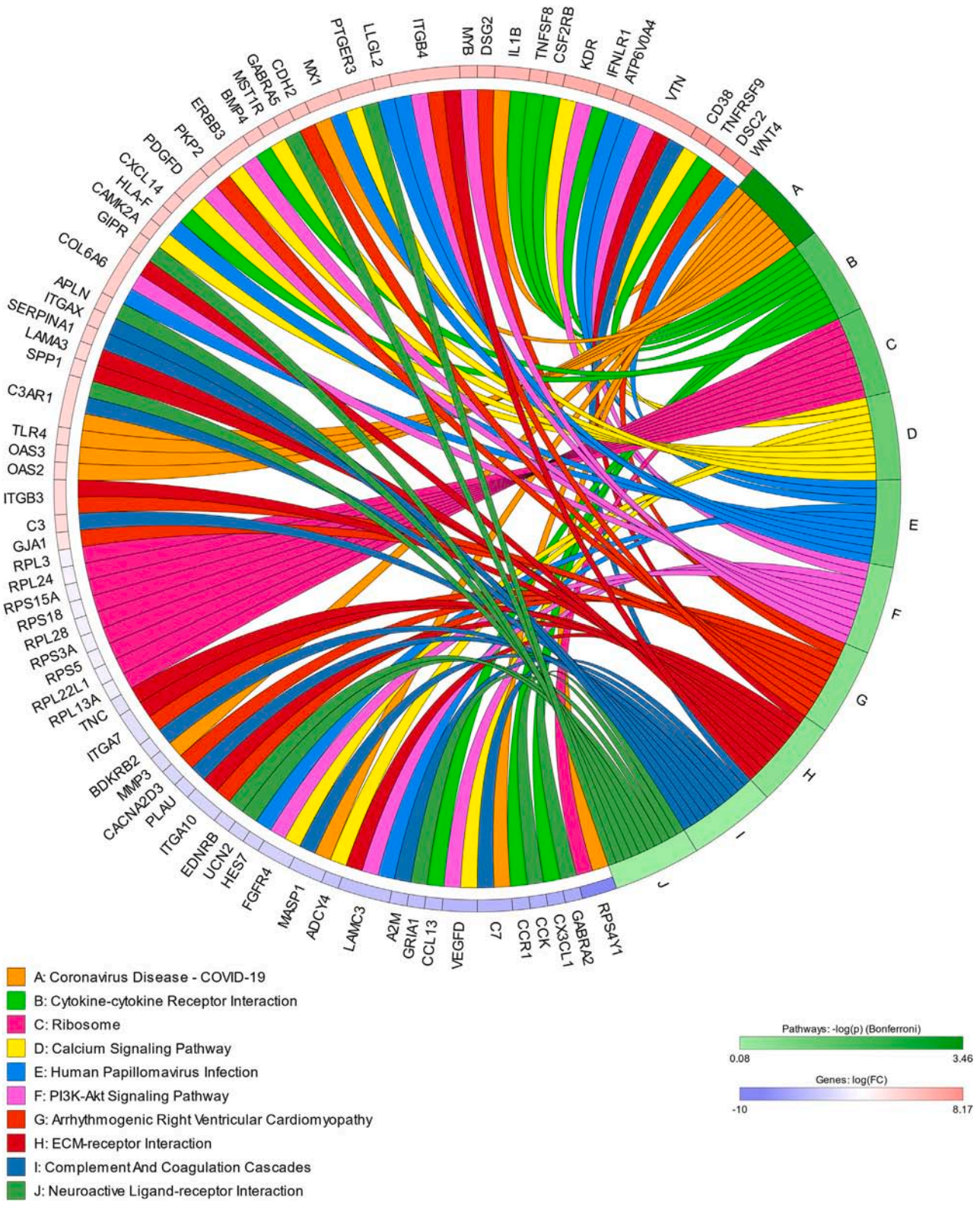

Figure 2. Top 10 most enriched pathways and the contributing DE genes

The pathways are labeled A to J, see the legend for the color of each pathway. For each pathway, the top 10 DE genes (with the lowest padj value) are shown. Note that several DE genes are contributing to more than one pathway.

Table 1. Hub genes determined by iPathwayGuide network analysis with a centrality degree (CD) above 0.20

Gene Symbol	Gene product	Centrality degree (CD)	*padj*	Log2FC
GNG4	G-protein subunit γ4	1.00	1.61E-03	2.92
C3[a]	Complement C3	0.71	1.41E-02	2.58
C3AR1[a]	Complement C3a receptor 1	0.45	6.90E-04	2.82
SERPINA1	α-1 antitrypsin (α-1 proteinase inhibitor)	0.36	3.32E-02	3.37
FPR1[a]	Formyl peptide receptor 1	0.36	2.00E-02	2.80
CCR1[a]	C-C motif chemokine receptor 1	0.35	3.78E-03	−6.37
CCL13[a]	C-C motif chemokine ligand 13	0.35	6.59E-03	−5.52
CX3CL1[a]	C-X3-C motif chemokine ligand 1 (fractalkine)	0.35	1.10E-04	−6.82
PTGER3[a]	Prostaglandin E receptor 3	0.35	3.94E-02	4.54
APLN[a]	Apelin	0.35	5.15E-04	3.47
PTGDR2[a]	Prostaglandin D2 receptor 2	0.35	4.52E-03	−4.00
SPP1	Osteopontin	0.31	4.90E-02	2.85
ITGB3	Integrin β3 subunit	0.31	1.00E-06	2.58
MSLN	Mesothelin (mucin 16)	0.31	1.72E-02	6.10
COL7A1	Collagen VII, α1 chain	0.29	1.00E-06	−4.20
BMP4	Bone morphogenetic protein 4	0.29	1.00E-06	4.23
CHRDL1	Chordin-like 1	0.29	1.00E-06	−6.23
CDH2	Cadherin-2	0.29	1.00E-06	4.43
EDNRA[a]	Endothelin receptor type A	0.27	1.54E-02	−2.57
EDNRB[a]	Endothelin receptor type B	0.27	1.29E-02	−3.38
COL5A3	Collagen V, α3 chain	0.25	3.00E-04	−3.55
TMEM132A	Transmembrane protein 132A	0.25	1.00E-06	3.34
ADRA1D[a]	Adrenoceptor α1D	0.24	7.38E-03	−2.72
KDR	Kinase insert domain receptor (VEGFR2)	0.24	1.00E-06	5.88
GPR4[a]	G protein-coupled receptor 4	0.24	4.26E-06	5.02
GPR143[a]	G protein-coupled receptor 143	0.24	3.90E-02	6.96
CCK[a]	Cholecystokinin	0.24	3.70E-04	−6.45
PLAU	Plasminogen activator, urokinase	0.22	1.00E-06	−3.19
COL15A1	Collagen XV, α1 chain	0.20	4.83E-03	−7.02
COL16A1	Collagen XVI, α1 chain	0.20	2.97E-05	−2.81
COL6A6	Collagen VI, α6 chain	0.20	4.63E-02	3.56

Genes are sorted on CD from highest to lowest.
[a]Denotes hub genes that are connected to GNG4, the hub gene with the highest CD and at the middle of the wheel network shown in Figure 2.

pericytes to PGE2 stimulation. Note that at baseline, cAMP levels were very low (1–2 pmol/mL) in both SScL and NORML pericytes. These data indicate that the altered expression profile of prostaglandin receptors in SSc lung pericytes negatively impacts cAMP production after receptor-mediated stimulation.

In further support of prostaglandin receptor changes, we found that PGE2 stimulation of NORML pericytes resulted in a significant decrease in the phosphorylation of AKT (pAKT) as compared to vehicle, consistent with signaling through the protective receptor PTGER2 (Figure 4D). By contrast, PGE2 stimulation of SSc lung pericytes did not exert a dampening effect on AKT phosphorylation, in contrast to the effect observed in normal pericytes. Thus, SSc lung pericytes and normal pericytes responded differently to PGE2 stimulation.

Perturbation of the PI3K-AKT signaling pathway

The PI3K-AKT pathway is one of the most enriched pathways in our systems level analysis (Table S4) containing 35 DE genes (Figure 5A). Four growth factors that activate receptor tyrosine kinases (RTKs) were differentially expressed in SSc lung pericytes, including VEGFD and EREG, which were downregulated, and PDGFD and EFNA1, which were upregulated (Figure 5A, orange stars). In the RTK family, *KDR*, *ERBB3*, *TEK*, and *FGFR3* were upregulated in SSc lung pericytes, while *FGFR4*, *PDGFRB*, and *KIT* were downregulated (Figure 5A, pink stars). The accumulation function of iPathwayGuide predicts that the total deregulation observed in these growth factors and RTKs would lead to the overall

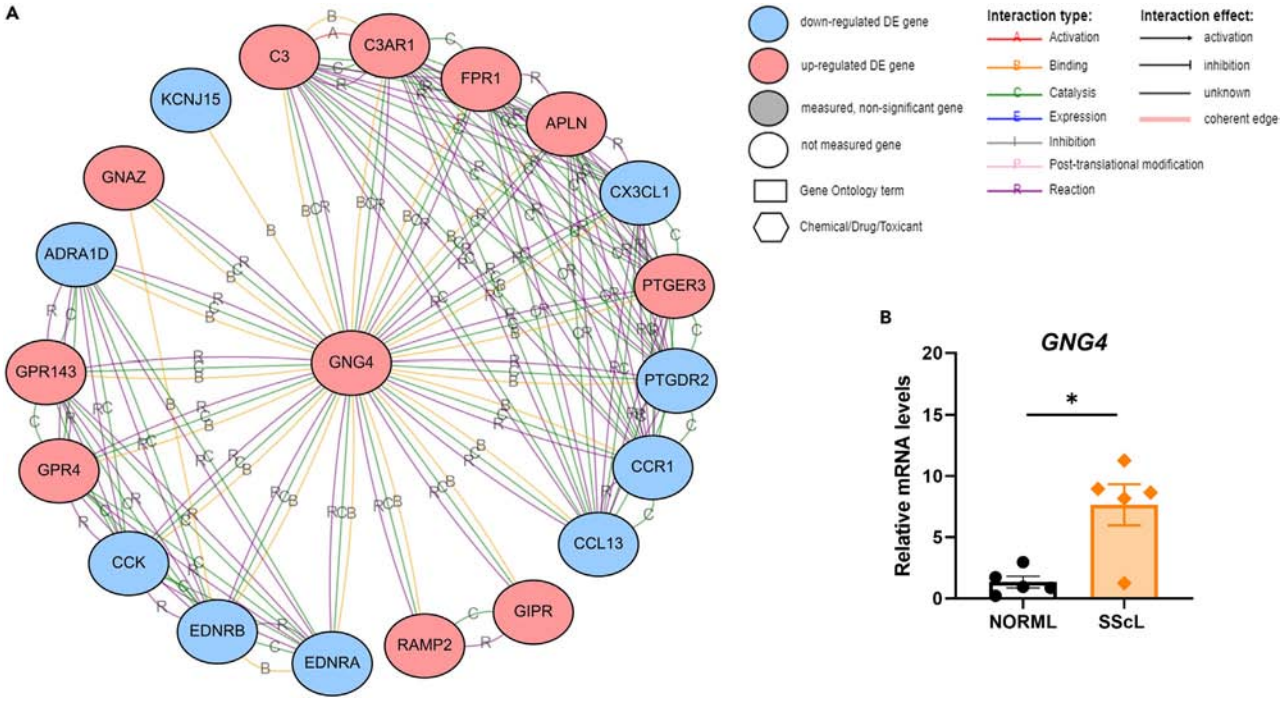

Figure 3. Network analysis

(A) The hub analysis revealed GNG4 at the center of the wheel network with the highest degree of centrality.

(B) GNG4 mRNA levels in SScL pericytes (n = 5) relative to NORML pericytes (n = 5). *p < 0.05 versus NORML (Mann-Whitney test). Data are represented as mean ± standard error of the mean (SEM).

downregulation of RTKs and the upregulation of genes in the axis *GRB2*→ *SOS1/2*→ *HRAS/KRAS/NRAS*→ *RAF1*→ *MAP2K1/2*→ *MAPK1/2* that is involved in cell proliferation, angiogenesis, and DNA repair processes (Figure 5B, green box). Both cell proliferation and angiogenesis biological processes were enriched in the GO analysis (Table S3).

Pericyte markers and angiogenesis factors

In addition to PDGFRβ, melanoma cell adhesion molecule (*MCAM*, aka CD146 and MUC18) has been used as a marker of pericytes, although marker positivity is variable in the lung.[25] We found that *MCAM* was upregulated in SSc lung pericytes, while *PDGFRB* was downregulated, suggesting changes in pericyte phenotype with disease. In addition, we found significant changes in genes involved in angiogenesis, including upregulation of *KDR* and *TEK* (which encode the receptors VEGFR2 and TIE2, respectively) and *APLN* (encoding apelin) and downregulation of *VEGFD* and *NES* (nestin)[26,27] (Figure 6A). As proof of concept, we confirmed downregulation of *VEGFD* by qPCR (Figure 6B). Taken together, these data demonstrate that the altered phenotype of SSc lung pericytes includes perturbation of vascular related pathways.

DISCUSSION

Persistent fibrosis and vascular dysfunction in the lung and other organs are key features of SSc. Given the central function of pericytes in maintaining capillary barrier function and integrity, as well as their demonstrated role in fibrosis, we surmised that these cells may be important in SSc-PF. Using an unbiased approach, we found that the transcriptome of pericytes isolated and cultured from SSc-PF lungs (SScL) significantly differs from that of pericytes from lungs without fibrotic disease (NORML). Over 1,000 genes were differentially expressed in SSc lung pericytes as compared to normal lung, with multiple pathways enriched in pericytes from fibrotic lung. GO analysis showed that biological processes related to cell adhesion and motility, cellular communication, ECM organization, angiogenesis, and G-protein coupled receptor signaling were among the most enriched in SSc lung pericytes as compared to NORML pericytes. Indeed, we found that *GNG4* is upregulated in SSc lung pericytes and is a central hub gene in a network that includes the prostaglandin receptors *PTGER3* and *PTGDR2*. We further showed that in response to the prostaglandin receptor ligand PGE2, SSc lung pericytes have decreased cAMP production and do not undergo downregulation of pAKT, unlike NORML pericytes. These results demonstrate functional significance of hub gene network perturbation. We also found that genes involved in PI3K-AKT signaling and angiogenesis were significantly altered in SSc lung pericytes, suggesting that these cells may impact the microvasculature in this disease.

When we constructed a network of hub genes with a high degree of centrality, *GNG4*, which encodes the γ4 subunit of guanine nucleotide binding protein (G protein), arose as a central node of a key regulatory network. We confirmed upregulation of *GNG4* expression in SSc lung

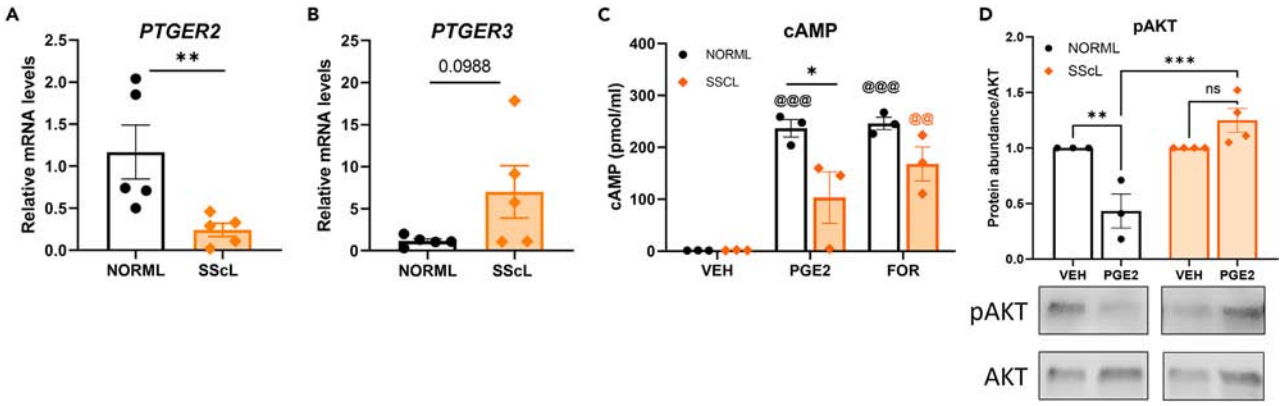

Figure 4. Validation experiments in SScL and NORML pericytes

(A and B) Transcript levels of (A) PTGER2 and (B) PTGER3 in SScL pericytes (n = 5) relative to NORML pericytes (n = 5).

(C) Levels of cAMP were measured in NORML (n = 3) and SScL (n = 3) pericytes treated with vehicle (VEH, 500 nM), PGE2 (500 nM), or forskolin (FOR, 100 mM) for 15 min.

(D) Protein abundance of pAKT normalized by total AKT in NORML (n = 3) and SScL (n = 4) pericytes treated with PGE2 and VEH. *p < 0.05, **p < 0.01, ***p < 0.001 as indicated by the lines; @ p < 0.05, @@ p < 0.01, @@@ p < 0.001 versus VEH-NORML (in black) or VEH-SScL (in orange). Data are represented as mean ± SEM.

pericytes relative to NORML by qPCR. To our knowledge, our study is the first to report expression of *GNG4* in human lung pericytes. *GNG4* is a member of the G-protein γ family, which relays signals from upstream G-protein-coupled receptors (GPCRs) to transduce extracellular signals from the environment into the cell.[28] In addition to GNG4, components of several GPCRs signaling pathways, including MAPK, PI3K and calcium signaling pathways, were also enriched in our analysis.[29] Under normal conditions, there is minimal detection of *GNG4* transcripts in the lung.[30] Interestingly, overexpression of *GNG4* expression is observed with many cancers, including breast, bladder, liver, gastric, and lung cancers, and is often associated with poorer prognosis.[31–35] Thus, upregulation of *GNG4* may be a marker of pathologic conditions.

We also found several key components of the prostaglandin signaling pathway that were deregulated in SSc lung pericytes: the PGE2 receptor *PTGER2* and the enzyme PTGS1 (aka *COX1*) were downregulated, while the PGE2 receptor *PTGER3* was upregulated. PTGS1, in conjunction with prostaglandin-endoperoxide synthase 2 (PTGS2, aka COX2), catalyzes the conversion of arachidonic acid into prostanoids including PGE2 and prostaglandin D2 (PGD2). While loss of PTGS2 has been associated with lung fibrosis,[36,37] the role that PTGS1 plays in SSc-PF remains uncharacterized. PGE2 signaling can impact lung inflammation and fibrosis via multiple mechanisms, including regulation of fibroblast proliferation, migration, collagen secretion, myofibroblast differentiation, Ca^{2+} oscillations, production of TNFα and MCP1 (aka CCL2), and the expression of ECM genes in idiopathic pulmonary fibrosis (IPF) cells and in TGFβ-treated lung fibroblasts.[38–41] PGE2 can bind to 4 different cell surface receptors, including PTGER2 and PTGER3. The signaling response to PGE2 depends on the relative binding to its different receptors.

PTGER2 (aka EP2) is categorized as a "relaxant receptor" (Figure 7). Under normal conditions, activation of PTGER2 initiates smooth muscle relaxation and activation of cAMP and PKA cascades that inhibit calcium waves and the PI3K/AKT signaling pathway.[38] Activation of PTGER2 confers protection against pulmonary fibrosis.[41–43] In contrast, PGE2 signaling through the "inhibitory receptor" PTGER3 (aka EP3) inhibits cAMP production and smooth muscle relaxation, as well as increases intracellular Ca^{2+} concentration.[44,45] The importance of the changes in relative expression of the different PGE2 receptors on SSc lung pericytes was demonstrated by their impaired production of cAMP in response to a brief PGE2 stimulation. In addition, we found that pAKT, which is normally downregulated by PGE2 signaling through EP2,[38] was either unchanged or even increased in SSc lung pericytes. Together, the downregulation of relaxant receptor *PTGER2* and upregulation of inhibitory receptor *PTGER3* in SSc lung pericytes could synergistically deplete cAMP and PKA reservoirs and impede the protective effect of PGE2 signaling in these cells by allowing more calcium waves and the activation of the PI3K-AKT pathway.[40]

SSc lung pericytes also exhibited a significant downregulation of *PTGDR2* compared to NORML cells. PTGDR2 (aka DP2 or CRTH2) is one of two G protein-coupled receptors that engage with PGD2 and modulate the production of Th2 cytokines by mast cells.[46] Initially recognized as a promising therapeutic target to treat allergic and asthmatic reactions,[47] PTGDR2 is now under investigation as a key player in other diseases, including lung fibrosis and inflammation.[48–50] PTGDR2 is expressed in most structural and immune cells of the human lung.[47] In mice, PTGDR2 deficiency exacerbated bleomycin-induced lung fibrosis.[50,51] Thus, the downregulation of *PTGDR2* in SSc lung pericytes may contribute to the progression of lung fibrosis.

We identified changes in expression of other hub genes of potential significance in fibrosis. Complement C3 (*C3*) and its receptor *C3AR1* were upregulated in SSc lung pericytes, and have been previously implicated in epithelial injury and fibrosis.[52] Osteopontin (*SPP1*), mesothelin (*MSLN*) and bone morphogenetic protein 4 are all profibrotic mediators whose expression was also increased in SSc lung pericytes.[53–55] Although the expression of several collagens was noted, we did not observe differential transcriptional changes in collagen I and III and

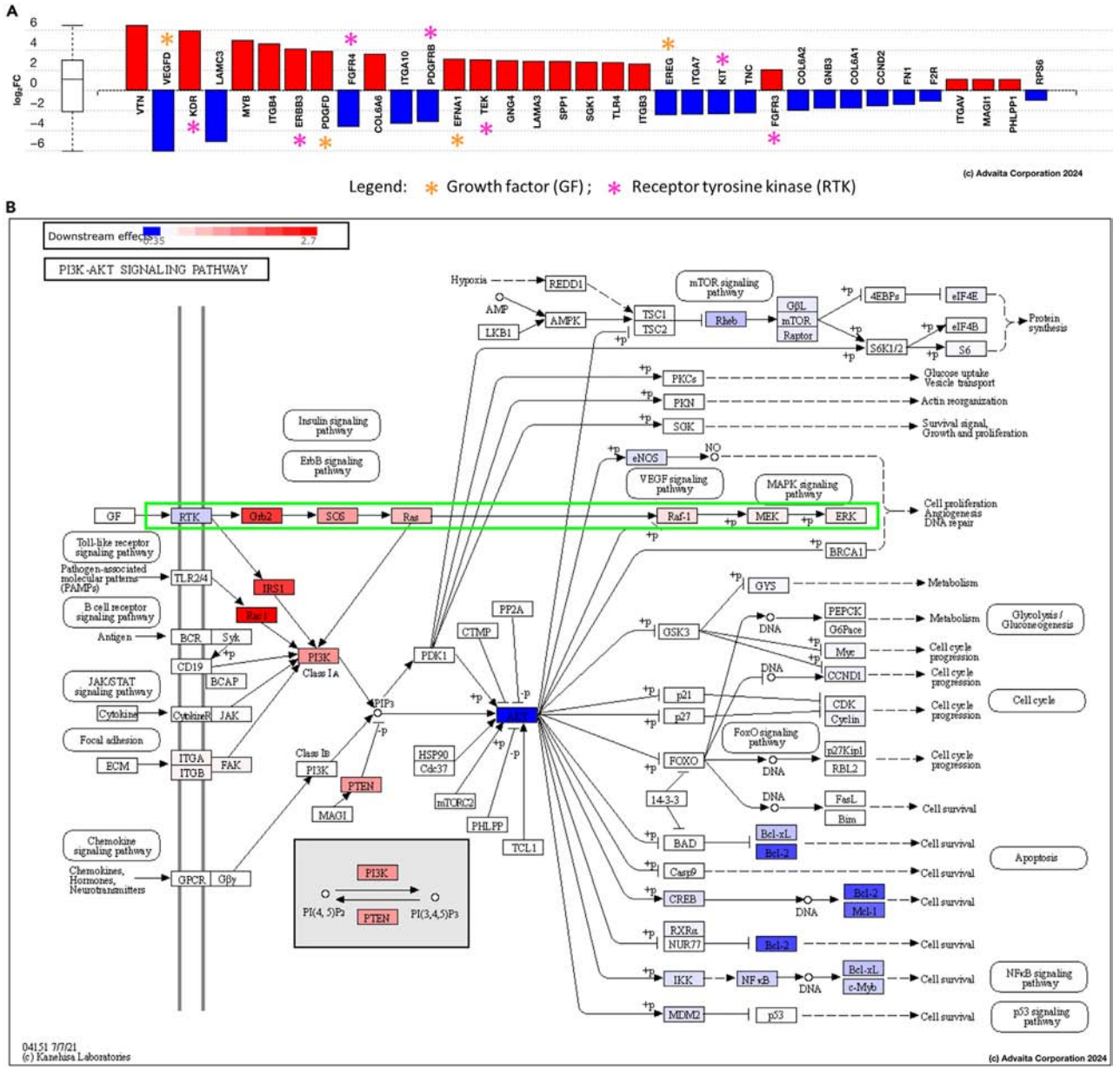

Figure 5. Enrichment of the PI3K-AKT signaling pathway

(A) DE genes from "SScL vs. NORML" comparison that are hit genes in the PI3K-AKT pathway. Orange star: growth factor (GF); pink star: receptor tyrosine kinase (RTK).

(B) Kyoto Encyclopedia of Genes and Genomes (KEGG) illustration of the PI3K-AKT pathway showing the accumulation prediction that iPathwayGuide generated based on the gene signature obtained in our differential expression analysis.

α-smooth muscle actin in SSc lung pericytes as compared to NORML. These results contrast with the findings by Valenzi et al., who documented an increase in *COL1A2* and *COL3A1* transcripts relative to control pericytes.[7] These conflicting data may be due to how tissues and cells were processed for RNA-seq, with both approaches having distinct advantages: Valenzi et al. assessed cells immediately from dissociated lung tissue, which will likely capture multiple populations of pericytes, including those that are activated or undergoing a myofibroblastic transition. For our analysis, cells were isolated and cultured in a medium that maintains pericyte identity and a relatively quiescent phenotype, allowing us to define the transcriptome of an enriched population of cells. In addition, the depth of RNA-seq data is increased by bulk analysis of cultured cells as compared to single-cell analysis, particularly for stromal cells, which are often under-represented in lung tissue digests.[22] Overall, our data indicate that SSc lung pericytes have been transcriptionally programmed to elaborate profibrotic mediators, suggesting that this may be another means by which these cells contribute to fibrosis.

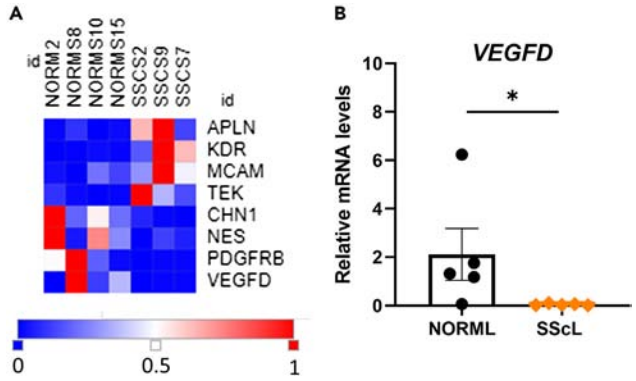

Figure 6. Deregulation of pericyte markers and angiogenesis factors in SScL pericytes

(A) Heatmap of differentially expressed pericyte markers and angiogenesis factors. Relative color scheme that uses the minimum and maximum values in each row to convert the values to color.

(B) VEGFD mRNA levels in SScL pericytes (n = 5) relative to NORML pericytes (n = 5). *p < 0.05 versus NORML (Mann-Whitney test). Data are represented as mean ± SEM.

The PI3K-AKT pathway plays a central role in the development of organ fibrosis by regulating a myriad of cellular functions such as cell cycle progression and proliferation, angiogenesis, DNA repair, cell survival and metabolism (glycolysis and gluconeogenesis).[56,57] The PI3K-AKT pathway is downstream of many other signaling pathways[57] that are also significantly enriched in our analysis, including focal adhesion, Ras, Rap1, cAMP, calcium and MAPK pathways. This pathway is also deregulated in IPF, and inhibition of PI3K/mTOR with the potent inhibitor omipalisib has been shown to ameliorate IPF in pre-clinical studies and clinical trials.[58,59]

We found other PI3K-AKT pathway-related genes whose expression was altered in SSc lung pericytes, including *PDGFRB* and genes associated with angiogenesis and vascular remodeling. Although both SSc and normal lung pericytes were selected based on PDGFRβ positivity, we detected decreased *PDGFRB* expression in SSc lung pericytes. *PDGFRB* downregulation is consistent with the reduction in PDGFRβ immunostaining observed in skin biopsies from SSc patients with late-stage disease.[60] Note that of the other canonical pericyte markers, only *MCAM* (CD146) expression was altered in SSc lung pericytes. Interestingly, we found in a previous study that a higher percentage of IPF pericytes vs. normal were positive for CD146.[17]

The decrease in *VEGFD* expression in SSc lung pericytes, which we verified by qPCR, was of particular interest, given that VEGFD mediates angiogenesis and is downregulated by TGFβ in human lung fibroblasts.[61] Expression of *APLN*, a hub gene connected to *GNG4*, was also increased: apelin not only stimulates angiogenesis[62] but also promotes vascular smooth muscle cell proliferation and migration.[63] Although both TIE2 (*TEK*) and VEGFR2 (*KDR*) are typical endothelial cell markers, both proteins have been detected at low levels on pericytes[12,13]; their upregulation on SSc lung pericytes may promote changes in angiopoietin and VEGF signaling. Alterations in the microvasculature are characteristic of SSc and include capillary regression, imbalances in angiogenesis, and structural abnormalities.[2] Taken together, our results suggest that the gene expression changes we identified in SSc lung pericytes could impact the vasculature in SSc-PF.

In conclusion, the basic markers that define pericytes are fundamentally similar in SSc lung pericytes compared to NORML, yet the gene expression signature of SSc lung pericytes is unique. The differential gene expression and pathways enriched in SSc lung pericytes implicate these cells in the fibrotic response and the vascular dysfunction that are defining features of SSc. Further studies will be needed to characterize the functional properties of SSc lung pericytes and explore other targets identified in our analysis.

Limitations of the study

There are some limitations to our study. The differential expression analysis was based on a relatively small number of SScL and NORML pericyte cell lines; for this reason, the samples were not explicitly age- or sex-matched. In addition, culturing these cells before transcriptomic analysis may not capture the full range of pericyte phenotypes that exist *in vivo*. Another caveat is that the SSc lung pericytes were isolated from the lungs of patients with severe disease; hence, the transcriptional changes we observed in SSc lung pericytes are reflective of advanced fibrosis and it is not known the extent to which these changes are intrinsic versus extrinsic (i.e., an influence of the fibrotic environment). Further studies are needed to characterize the functional properties of SSc lung pericytes, to explore other targets identified in our analysis, and to correlate gene expression differences with protein.

STAR★METHODS

Detailed methods are provided in the online version of this paper and include the following:

- KEY RESOURCES TABLE
- RESOURCE AVAILABILITY
  - Lead contact

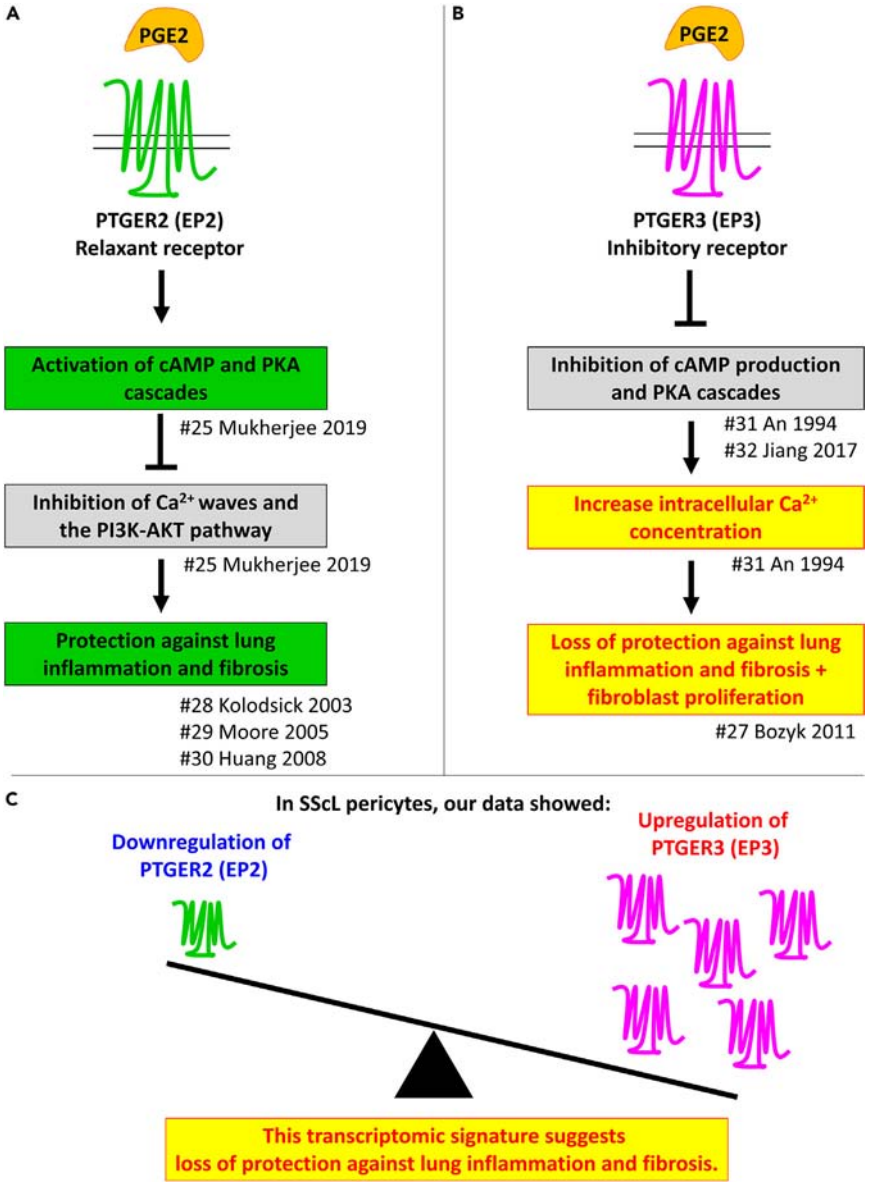

Figure 7. Role of PTGER2 and PTGER3 in lung inflammation and fibrosis

(A) Under normal conditions, activation of PTGER2 (aka EP2) by PGE2 initiates activation of cAMP and PKA cascades that inhibit calcium waves and the PI3K/AKT signaling pathway,[38] thus conferring protection against pulmonary inflammation and fibrosis.[41–43]

(B) In contrast, PGE2 signaling through PTGER3 (aka EP3) inhibits cAMP production and increases intracellular Ca^{2+} concentration.[44,45]

(C) The transcriptomic signature we observed in our RNA-seq analysis revealed that PTGER2 is downregulated and PTGER3 is upregulated in SScL pericytes, a signature that has been shown to lead to the loss of protection against lung inflammation and fibrosis.

- cAMP assay and pAKT/AKT Westerns
- QUANTIFICATION AND STATISTICAL ANALYSIS

SUPPLEMENTAL INFORMATION

Supplemental information can be found online at https://doi.org/10.1016/j.isci.2024.110010.

ACKNOWLEDGMENTS

We acknowledge Benjamin Simon, Shota Yamamoto, and Alec Morlote for technical assistance. This research was funded by the National Institutes of Health grants R01 HL133751 (to L.M.S. and C.A.F.-B.), K24 AR060297 (to C.A.F.-B.), R01 HL153195 (to C.A.F.-B.) and T32 AR050958 (to L.R.).

AUTHOR CONTRIBUTIONS

C.L.W., L.M.S., and C.A.F.-B. conceived and designed research, C.L.W. and L.R. performed experiments, C.L.W. and L.R. analyzed data, C.L.W., L.R., R.L., L.M.S., and C.A.F.-B. interpreted results of experiments, C.L.W. and L.R. prepared figures, C.L.W. and L.R. drafted manuscript, C.L.W., L.R., R.L., L.M.S., and C.A.F.-B. edited and revised manuscript, C.L.W., L.R., R.L., L.M.S., and C.A.F.-B. approved the final version of manuscript.

DECLARATION OF INTERESTS

The authors declare no competing interests.

Received: July 11, 2023
Revised: February 9, 2024
Accepted: May 14, 2024
Published: May 17, 2024

REFERENCES

1. Denton, C.P., and Khanna, D. (2017). Systemic sclerosis. Lancet *390*, 1685–1699.
2. Trojanowska, M. (2010). Cellular and molecular aspects of vascular dysfunction in systemic sclerosis. Nat. Rev. Rheumatol. *6*, 453–460.
3. Steen, V.D., and Medsger, T.A. (2007). Changes in causes of death in systemic sclerosis, 1972–2002. Ann. Rheum. Dis. *66*, 940–944.
4. Armulik, A., Genové, G., and Betsholtz, C. (2011). Pericytes: developmental, physiological, and pathological perspectives, problems, and promises. Dev. Cell *21*, 193–215.
5. Fleming, J.N., Nash, R.A., McLeod, D.O., Fiorentino, D.F., Shulman, H.M., Connolly, M.K., Molitor, J.A., Henstorf, G., Lafyatis, R., Pritchard, D.K., et al. (2008). Capillary regeneration in scleroderma: stem cell therapy reverses phenotype? PLoS One *3*, e1452.
6. Helmbold, P., Fiedler, E., Fischer, M., and Marsch, W.C. (2004). Hyperplasia of dermal microvascular pericytes in scleroderma. J. Cutan. Pathol. *31*, 431–440.
7. Valenzi, E., Bulik, M., Tabib, T., Morse, C., Sembrat, J., Trejo Bittar, H., Rojas, M., and Lafyatis, R. (2019). Single-cell analysis reveals fibroblast heterogeneity and myofibroblasts in systemic sclerosis-associated interstitial lung disease. Ann. Rheum. Dis. *78*, 1379–1387.
8. Liakouli, V., Cipriani, P., Di Benedetto, P., Ruscitti, P., Carubbi, F., Berardicurti, O., Panzera, N., and Giacomelli, R. (2018). The role of extracellular matrix components in angiogenesis and fibrosis: Possible implication for Systemic Sclerosis. Mod. Rheumatol. *28*, 922–932. https://doi.org/10.1080/14397595.2018.1431004.
9. Distler, O., del Rosso, A., Giacomelli, R., Cipriani, P., Conforti, M.L., Guiducci, S., Gay, R.E., Michel, B.A., Brühlmann, P., Müller-Ladner, U., et al. (2002). Angiogenic and angiostatic factors in systemic sclerosis: increased levels of vascular endothelial growth factor are a feature of the earliest disease stages and are associated with the absence of fingertip ulcers. Arthritis Res. *4*, R11. https://doi.org/10.1186/ar596.
10. Sweeney, M., and Foldes, G. (2018). It takes two: endothelial-perivascular cell cross-talk in vascular development and disease. Front. Cardiovasc. Med. *5*, 154.
11. Eilken, H.M., Diéguez-Hurtado, R., Schmidt, I., Nakayama, M., Jeong, H.-W., Arf, H., Adams, S., Ferrara, N., and Adams, R.H. (2017). Pericytes regulate VEGF-induced endothelial sprouting through VEGFR1. Nat. Commun. *8*, 1574.
12. Gong, C.-X., Zhang, Q., Xiong, X.-Y., Yuan, J.-J., Yang, G.-Q., Huang, J.-C., Liu, J., Duan, C.-M., Rui-Xu, Qiu, Z.M., et al. (2021). Pericytes regulate cerebral perfusion through VEGFR1 in ischemic stroke. Cell. Mol. Neurobiol. *42*, 1897–1908.
13. Teichert, M., Milde, L., Holm, A., Stanicek, L., Gengenbacher, N., Savant, S., Ruckdeschel, T., Hasanov, Z., Srivastava, K., Hu, J., et al. (2017). Pericyte-expressed Tie2 controls angiogenesis and vessel maturation. Nat. Commun. *8*, 16106.
14. Dulauroy, S., Di Carlo, S.E., Langa, F., Eberl, G., and Peduto, L. (2012). Lineage tracing and genetic ablation of ADAM12+ perivascular cells identify a major source of profibrotic cells during acute tissue injury. Nat. Med. *18*, 1262–1270. https://doi.org/10.1038/nm.2848.
15. Humphreys, B.D., Lin, S.-L., Kobayashi, A., Hudson, T.E., Nowlin, B.T., Bonventre, J.V., Valerius, M.T., McMahon, A.P., and Duffield, J.S. (2010). Fate tracing reveals the pericyte and not epithelial origin of myofibroblasts in kidney fibrosis. Am. J. Pathol. *176*, 85–97.
16. Hung, C., Linn, G., Chow, Y.-H., Kobayashi, A., Mittelsteadt, K., Altemeier, W.A., Gharib, S.A., Schnapp, L.M., and Duffield, J.S. (2013). Role of lung pericytes and resident fibroblasts in the pathogenesis of pulmonary fibrosis. Am. J. Respir. Crit. Care Med. *188*, 820–830.
17. Wilson, C.L., Stephenson, S.E., Higuero, J.P., Feghali-Bostwick, C., Hung, C.F., and Schnapp, L.M. (2018). Characterization of human PDGFR-β-positive pericytes from IPF and non-IPF lungs. Am. J. Physiol. Lung Cell Mol. Physiol. *315*, L991–L1002.
18. Rajkumar, V.S., Howell, K., Csiszar, K., Denton, C.P., Black, C.M., and Abraham, D.J. (2005). Shared expression of phenotypic markers in systemic sclerosis indicates a convergence of pericytes and fibroblasts to a myofibroblast lineage in fibrosis. Arthritis Res. Ther. *7*, R1113–R1123. https://doi.org/10.1186/ar1790.
19. Garrett, S.M., Baker Frost, D., and Feghali-Bostwick, C. (2017). The mighty fibroblast and its utility in scleroderma research. J. Scleroderma Relat. Disord. *2*, 69–134.
20. Rosa, I., Romano, E., Fioretto, B.S., and Manetti, M. (2020). The contribution of mesenchymal transitions to the pathogenesis of systemic sclerosis. Eur. J. Rheumatol. *7*, S157–S164. https://doi.org/10.5152/eurjrheum.2019.19081.
21. Talotta, R., Atzeni, F., Ditto, M.C., Gerardi, M.C., Batticciotto, A., Bongiovanni, S., and Puttini, P.S. (2018). Certainties and uncertainties concerning the contribution of

pericytes to the pathogenesis of systemic sclerosis. J. Scleroderma Relat. Disord. *3*, 14–20. https://doi.org/10.5301/jsrd.5000254.

22. Koenitzer, J.R., Wu, H., Atkinson, J.J., Brody, S.L., and Humphreys, B.D. (2020). Single-nucleus RNA-sequencing profiling of mouse lung. Reduced dissociation bias and improved rare cell-type detection compared with single-cell RNA sequencing. Am. J. Respir. Cell Mol. Biol. *63*, 739–747.
23. Bagley, R.G., Rouleau, C., Morgenbesser, S.D., Weber, W., Cook, B.P., Shankara, S., Madden, S.L., and Teicher, B.A. (2006). Pericytes from human non-small cell lung carcinomas: an attractive target for anti-angiogenic therapy. Microvasc. Res. *71*, 163–174.
24. Rustenhoven, J., Smyth, L.C., Jansson, D., Schweder, P., Aalderink, M., Scotter, E.L., Mee, E.W., Faull, R.L.M., Park, T.I.-H., and Dragunow, M. (2018). Modelling physiological and pathological conditions to study pericyte biology in brain function and dysfunction. BMC Neurosci. *19*, 6–15.
25. Hung, C.F., Wilson, C.L., and Schnapp, L.M. (2019). Pericytes in the lung. Adv. Exp. Med. Biol. *1122*, 41–58.
26. Tsigkos, S., Koutsilieris, M., and Papapetropoulos, A. (2003). Angiopoietins in angiogenesis and beyond. Expet Opin. Invest. Drugs *12*, 933–941.
27. Tan, S., Chen, Y., Du, S., Li, W., Liu, P., Zhao, J., Yang, P., Cai, J., Gao, R., and Wang, Z. (2022). TIE2-high cervical cancer cells promote tumor angiogenesis by upregulating TIE2 and VEGFR2 in endothelial cells. Transl. Oncol. *26*, 101539.
28. Hepler, J.R., and Gilman, A.G. (1992). G proteins. Trends Biochem. Sci. *17*, 383–387.
29. Pal, J., Patil, V., Mondal, B., Shukla, S., Hegde, A.S., Arivazhagan, A., Santosh, V., and Somasundaram, K. (2016). Epigenetically silenced GNG4 inhibits SDF1α/CXCR4 signaling in mesenchymal glioblastoma. Genes Cancer *7*, 136–147. https://doi.org/10.18632/genesandcancer.105.
30. Karlsson, M., Zhang, C., Méar, L., Zhong, W., Digre, A., Katona, B., Sjöstedt, E., Butler, L., Odeberg, J., Dusart, P., et al. (2021). A single-cell type transcriptomics map of human tissues. Sci. Adv. *7*, eabh2169. https://doi.org/10.1126/sciadv.abh2169.
31. Uhlen, M., Zhang, C., Lee, S., Sjöstedt, E., Fagerberg, L., Bidkhori, G., Benfeitas, R., Arif, M., Liu, Z., Edfors, F., et al. (2017). A pathology atlas of the human cancer transcriptome. Science *357*, eaan2507. https://doi.org/10.1126/science.aan2507.
32. Zhu, D., Gu, X., Lin, Z., Yu, D., and Wang, J. (2021). High expression of PSMC2 promotes gallbladder cancer through regulation of GNG4 and predicts poor prognosis. Oncogenesis *10*, 43.
33. Zhao, H., Sheng, D., Qian, Z., Ye, S., Chen, J., and Tang, Z. (2021). Identifying GNG4 might play an important role in colorectal cancer TMB. Cancer Biomarkers *32*, 435–450.
34. Zhang, X., Kang, X., Jin, L., Bai, J., Zhang, H., Liu, W., and Wang, Z. (2020). ABCC9, NKAPL, and TMEM132C are potential diagnostic and prognostic markers in triple-negative breast cancer. Cell Biol. Int. *44*, 2002–2010.
35. Tanaka, H., Kanda, M., Miwa, T., Umeda, S., Sawaki, K., Tanaka, C., Kobayashi, D., Hayashi, M., Yamada, S., Nakayama, G., et al. (2021). G-protein subunit gamma-4 expression has potential for detection, prediction and therapeutic targeting in liver metastasis of gastric cancer. Br. J. Cancer *125*, 220–228.
36. Coward, W.R., Feghali-Bostwick, C.A., Jenkins, G., Knox, A.J., and Pang, L. (2014). A central role for G9a and EZH2 in the epigenetic silencing of cyclooxygenase-2 in idiopathic pulmonary fibrosis. Faseb. J. *28*, 3183–3196.
37. Keerthisingam, C.B., Jenkins, R.G., Harrison, N.K., Hernandez-Rodriguez, N.A., Booth, H., Laurent, G.J., Hart, S.L., Foster, M.L., and McAnulty, R.J. (2001). Cyclooxygenase-2 deficiency results in a loss of the anti-proliferative response to transforming growth factor-β in human fibrotic lung fibroblasts and promotes bleomycin-induced pulmonary fibrosis in mice. Am. J. Pathol. *158*, 1411–1422.
38. Mukherjee, S., Sheng, W., Michkov, A., Sriarm, K., Sun, R., Dvorkin-Gheva, A., Insel, P.A., and Janssen, L.J. (2019). Prostaglandin E_2 inhibits profibrotic function of human pulmonary fibroblasts by disrupting Ca^{2+} signaling. Am. J. Physiol. Lung Cell Mol. Physiol. *316*, L810–L821.
39. Kida, T., Ayabe, S., Omori, K., Nakamura, T., Maehara, T., Aritake, K., Urade, Y., and Murata, T. (2016). Prostaglandin D2 attenuates bleomycin-induced lung inflammation and pulmonary fibrosis. PLoS One *11*, e0167729.
40. Bozyk, P.D., and Moore, B.B. (2011). Prostaglandin E2 and the pathogenesis of pulmonary fibrosis. Am. J. Respir. Cell Mol. Biol. *45*, 445–452.
41. Kolodsick, J.E., Peters-Golden, M., Larios, J., Toews, G.B., Thannickal, V.J., and Moore, B.B. (2003). Prostaglandin E2 Inhibits Fibroblast to Myofibroblast Transition via E. Prostanoid Receptor 2 Signaling and Cyclic Adenosine Monophosphate Elevation. Am. J. Respir. Cell Mol. Biol. *29*, 537–544. https://doi.org/10.1165/rcmb.2002-0243OC.
42. Moore, B.B., Ballinger, M.N., White, E.S., Green, M.E., Herrygers, A.B., Wilke, C.A., Toews, G.B., and Peters-Golden, M. (2005). Bleomycin-induced E prostanoid receptor changes alter fibroblast responses to prostaglandin E2. J. Immunol. *174*, 5644–5649.
43. Huang, S.K., Wettlaufer, S.H., Chung, J., and Peters-Golden, M. (2008). Prostaglandin E2 inhibits specific lung fibroblast functions via selective actions of PKA and Epac-1. Am. J. Respir. Cell Mol. Biol. *39*, 482–489.
44. An, S., Yang, J., So, S.W., Zeng, L., and Goetzl, E.J. (1994). Isoforms of the EP3 subtype of human prostaglandin E2 receptor transduce both intracellular calcium and cAMP signals. Biochemistry *33*, 14496–14502.
45. Jiang, J., Qiu, J., Li, Q., and Shi, Z. (2017). Prostaglandin E2 Signaling: Alternative Target for Glioblastoma? Trends Cancer *3*, 75–78. https://doi.org/10.1016/j.trecan.2016.12.002.
46. Xue, L., Barrow, A., and Pettipher, R. (2009). Interaction between prostaglandin D and chemoattractant receptor-homologous molecule expressed on Th2 cells mediates cytokine production by Th2 lymphocytes in response to activated mast cells. Clin. Exp. Immunol. *156*, 126–133. https://doi.org/10.1111/j.1365-2249.2008.03871.x.
47. Jandl, K., and Heinemann, A. (2017). The therapeutic potential of CRTH2/DP2 beyond allergy and asthma. Prostag. Other Lipid Mediat. *133*, 42–48. https://doi.org/10.1016/j.prostaglandins.2017.08.006.
48. Boin, F., De Fanis, U., Bartlett, S.J., Wigley, F.M., Rosen, A., and Casolaro, V. (2008). T cell polarization identifies distinct clinical phenotypes in scleroderma lung disease. Arthritis Rheum. *58*, 1165–1174. https://doi.org/10.1002/art.23406.
49. Thrall, R.S., McCormick, J.R., Jack, R.M., McReynolds, R.A., and Ward, P.A. (1979). Bleomycin-induced pulmonary fibrosis in the rat: inhibition by indomethacin. Am. J. Pathol. *95*, 117–130.
50. Ueda, S., Fukunaga, K., Takihara, T., Shiraishi, Y., Oguma, T., Shiomi, T., Suzuki, Y., Ishii, M., Sayama, K., Kagawa, S., et al. (2019). Deficiency of $CRTH_2$, a Prostaglandin D_2 Receptor, Aggravates Bleomycin-induced Pulmonary Inflammation and Fibrosis. Am. J. Respir. Cell Mol. Biol. *60*, 289–298. https://doi.org/10.1165/rcmb.2017-0397OC.
51. Kurosaki, F., Uchibori, R., Sehara, Y., Saga, Y., Urabe, M., Mizukami, H., Hagiwara, K., and Kume, A. (2018). AAV6-Mediated IL-10 Expression in the lung ameliorates bleomycin-induced pulmonary fibrosis in mice. Hum. Gene Ther. *29*, 1242–1251.
52. Gu, H., Fisher, A.J., Mickler, E.A., Duerson, F., 3rd, Cummings, O.W., Peters-Golden, M., Twigg, H.L., 3rd, Woodruff, T.M., Wilkes, D.S., and Vittal, R. (2016). Contribution of the anaphylatoxin receptors, C3aR and C5aR, to the pathogenesis of pulmonary fibrosis. Faseb. J. *30*, 2336–2350.
53. Pardo, A., Gibson, K., Cisneros, J., Richards, T.J., Yang, Y., Becerril, C., Yousem, S., Herrera, I., Ruiz, V., Selman, M., and Kaminski, N. (2005). Up-regulation and profibrotic role of osteopontin in human idiopathic pulmonary fibrosis. PLoS Med. *2*, e251.
54. Nishio, T., Koyama, Y., Fuji, H., Ishizuka, K., Iwaisako, K., Taura, K., Hatano, E., Brenner, D.A., and Kisseleva, T. (2022). The Role of Mesothelin in Activation of Portal Fibroblasts in Cholestatic Liver Injury. Biology *11*, 1589.
55. Yang, M., and Zhang, C. (2021). The role of bone morphogenetic proteins in liver fibrosis. Gastroenterol. Hepatol. Open Access *12*, 17–20.
56. Cantley, L.C. (2002). The phosphoinositide 3-kinase pathway. Science *296*, 1655–1657.
57. Yan, Z., kui, Z., and Ping, Z. (2014). Reviews and prospectives of signaling pathway analysis in idiopathic pulmonary fibrosis. Autoimmun. Rev. *13*, 1020–1025. https://doi.org/10.1016/j.autrev.2014.08.028.
58. Mercer, P.F., Woodcock, H.V., Eley, J.D., Platé, M., Sulikowski, M.G., Durrenberger, P.F., Franklin, L., Nanthakumar, C.B., Man, Y., Genovese, F., et al. (2016). Exploration of a potent PI3 kinase/mTOR inhibitor as a novel anti-fibrotic agent in IPF. Thorax *71*, 701–711.
59. Lukey, P.T., Harrison, S.A., Yang, S., Man, Y., Holman, B.F., Rashidnasab, A., Azzopardi, G., Grayer, M., Simpson, J.K., Bareille, P., et al. (2019). A randomised, placebo-controlled study of omipalisib (PI3K/mTOR) in idiopathic pulmonary fibrosis. Eur. Respir. J. *53*, 1801992. https://doi.org/10.1183/13993003.01992-2018.
60. Rajkumar, V.S., Sundberg, C., Abraham, D.J., Rubin, K., and Black, C.M. (1999). Activation of microvascular pericytes in autoimmune Raynaud's phenomenon and systemic sclerosis. Arthritis Rheum. *42*, 930–941.
61. Cui, Y., Osorio, J.C., Risquez, C., Wang, H., Shi, Y., Gochuico, B.R., Morse, D., Rosas, I.O., and El-Chemaly, S. (2014). Transforming growth factor-β1 downregulates vascular endothelial growth factor-D expression in human lung fibroblasts via the Jun

NH2-terminal kinase signaling pathway. Mol. Med. *20*, 120–134.

62. Kasai, A., Shintani, N., Oda, M., Kakuda, M., Hashimoto, H., Matsuda, T., Hinuma, S., and Baba, A. (2004). Apelin is a novel angiogenic factor in retinal endothelial cells. Biochem. Biophys. Res. Commun. *325*, 395–400.
63. Li, F., Li, L., Qin, X., Pan, W., Feng, F., Chen, F., Zhu, B., Liao, D., Tanowitz, H., Albanese, C., and Chen, L. (2008). Apelin-induced vascular smooth muscle cell proliferation: the regulation of cyclin D1. Front. Biosci. *13*, 3786–3792.
64. Nguyen, X.-X., Renaud, L., and Feghali-Bostwick, C. (2021). Identification of Impacted Pathways and Transcriptomic Markers as Potential Mediators of Pulmonary Fibrosis in Transgenic Mice Expressing Human IGFBP5. Int. J. Mol. Sci. *22*, 12609.
65. Love, M.I., Huber, W., and Anders, S. (2014). Moderated estimation of fold change and dispersion for RNA-seq data with DESeq2. Genome Biol. *15*, 550.
66. Malaab, M., Renaud, L., Takamura, N., Zimmerman, K.D., da Silveira, W.A., Ramos, P.S., Haddad, S., Peters-Golden, M., Penke, L.R., Wolf, B., et al. (2022). Antifibrotic factor KLF4 is repressed by the miR-10/TFAP2A/TBX5 axis in dermal fibroblasts: insights from twins discordant for systemic sclerosis. Ann. Rheum. Dis. *81*, 268–277.
67. Kanehisa, M., Goto, S., Kawashima, S., and Nakaya, A. (2002). The KEGG databases at GenomeNet. Nucleic Acids Res. *30*, 42–46.
68. Gene Ontology Consortium (2001). Creating the gene ontology resource: design and implementation. Genome Res. *11*, 1425–1433.
69. Draghici, S., Khatri, P., Tarca, A.L., Amin, K., Done, A., Voichita, C., Georgescu, C., and Romero, R. (2007). A systems biology approach for pathway level analysis. Genome Res. *17*, 1537–1545.
70. Tarca, A.L., Draghici, S., Khatri, P., Hassan, S.S., Mittal, P., Kim, J.-S., Kim, C.J., Kusanovic, J.P., and Romero, R. (2009). A novel signaling pathway impact analysis. Bioinformatics *25*, 75–82.
71. Khatri, P., Draghici, S., Tarca, A.L., Hassan, S.S., and Romero, R. (2007). A System Biology Approach for the Steady-State Analysis of Gene Signaling Networks (Springer), pp. 32–41.
72. Nguyen, T.-M., Shafi, A., Nguyen, T., and Draghici, S. (2019). Identifying significantly impacted pathways: a comprehensive review and assessment. Genome Biol. *20*, 203.
73. Chen, J., Bardes, E.E., Aronow, B.J., and Jegga, A.G. (2009). ToppGene Suite for gene list enrichment analysis and candidate gene prioritization. Nucleic Acids Res. *37*, W305–W311.
74. Supek, F., Bošnjak, M., Škunca, N., and Šmuc, T. (2011). REVIGO summarizes and visualizes long lists of gene ontology terms. PLoS One *6*, e21800.

STAR★METHODS

KEY RESOURCES TABLE

REAGENT or RESOURCE	SOURCE	IDENTIFIER
Antibodies		
phospho AKT (Ser-473)	Cell Signaling	Cat#9271; RRID: AB_329825
total AKT	Cell Signaling	Cat#9272; RRID: AB_329827
Biological samples		
NORM2	CFB cryobank	NORML
NORMS7	CFB cryobank	NORML
NORMS8	CFB cryobank	NORML
NORMS10	CFB cryobank	NORML
NORMS13	CFB cryobank	NORML
NORMS15	CFB cryobank	NORML
NORMS20	CFB cryobank	NORML
SSCS2	CFB cryobank	SScL
SSCS4	CFB cryobank	SScL
SSCS7	CFB cryobank	SScL
SSCS9	CFB cryobank	SScL
SSCS10	CFB cryobank	SScL
SSCS11	CFB cryobank	SScL
SSCS12	CFB cryobank	SScL
Chemicals, peptides, and recombinant proteins		
PGE2	Cayman Chemical	Cat#363-24-6
Forskolin	BioVision EZSolution	Cat#26625
Critical commercial assays		
Parameter Competitive cAMP Assay	R&D Systems, Inc. Minneapolis, MN	Cat#KGE002B
Aurum™ Total RNA Mini kit	Bio-Rad, Hercules, CA	Cat#7326820
iScript Reverse Transcription SuperMix	Bio-Rad, Hercules, CA	Cat#1708840
SsoAdvanced Universal Probes Supermix	Bio-Rad, Hercules, CA	Cat#1725284
ANGPT1	Applied Biosystems	Hs00375822_m1
B2M	Applied Biosystems	Hs00187842_m1
FIGF (aka *VEGFD*)	Applied Biosystems	Hs01128659_m1
GNG4	Applied Biosystems	Hs00189551_m1
MYH11	Applied Biosystems	Hs00224610_m1
PTGER2	Applied Biosystems	Hs00168754_m1
PTGER3	Applied Biosystems	Hs00168755_m1
Deposited data		
RNAseq data	NCBI GEO	GEO: GSE222552
Western blots (original)	Figshare	https://doi.org/10.6084/m9.figshare.25646856.v1
Supplemental Figures and Tables	Figshare	https://doi.org/10.6084/m9.figshare.25758417.v1
Software and algorithms		
iPathwayGuide (Advaita)	https://advaitabio.com/	N/A
ImageJ	https://imagej.net/	N/A
DESeq2 R package	https://rdrr.io/bioc/DESeq2/	N/A

(*Continued on next page*)

Continued

REAGENT or RESOURCE	SOURCE	IDENTIFIER
ToppFun (ToppGene Suite)	https://toppgene.cchmc.org/enrichment.jsp	N/A
GraphPad Prism	GraphPad Software, CA	version 9 for Windows

RESOURCE AVAILABILITY

Lead contact

Further information and requests for resources and reagents should be directed to and will be fulfilled by the lead contact, Dr. Carol Feghali-Bostwick (feghalib@musc.edu).

Materials availability

This study did not generate new unique reagents.

Data and code availability

- The RNA-seq data has been deposited at NCBI GEO: GSE222552 and is now publicly accessible. Accession numbers are listed in the key resources table. Original western blot images have been deposited at Figshare and are publicly available as of the date of publication. The DOI is listed in the key resources table. Microscopy data reported in this paper will be shared by the lead contact upon request. Any additional information required to reanalyze the data reported in this paper is available from the lead contact upon request.
- This paper does not report original code.
- Any additional information required to reanalyze the data reported in this paper is available from the lead contact upon request.

EXPERIMENTAL MODEL AND STUDY PARTICIPANT DETAILS

Primary cultures of lung pericytes

Lung explants from SSc patients with severe pulmonary fibrosis ("SScL", n=7) were obtained from the University of Pittsburgh. Lungs from rejected organ donors with no clinical history of lung disease were also obtained from the University of Pittsburgh and designated as normal in this study ("NORML", n=7). This study was approved by the Institutional Review Board of the University of Pittsburgh under protocol# 970946. This study is deemed as non-human subject research by the MUSC Institutional Review Board because human lung tissues were received without any identifiers.

Tissue was processed for cell culture at 37°C and selection of PDGFRβ+ cells as described previously.[17] Briefly, minced and enzymatically digested lung tissue was plated on 0.2% gelatin-coated dishes in a specialized, low-serum (2% FBS) medium conducive for pericyte growth (Pericyte Medium; ScienCell, Carlsbad, CA, catalog #1201). After expansion of the cells in Pericyte Medium (generally for 10-20 days), cells were used for antibody-based magnetic bead selection (Miltenyi). After depletion of cells positive for CD45 (leukocytes), CD31 (PECAM; endothelial cells), and CD326 (EpCAM; epithelial cells), the remaining cells were labeled with PE-conjugated anti-PDGFRβ (Miltenyi, clone REA363) for positive selection. PDGFRβ+ cells were cultured in Pericyte Medium for up to 8 passages. NORML and SScL pericytes in culture displayed a morphology consistent with pericytes (spindle shaped with elongated cellular processes; Figure S2A) and could be readily distinguished from normal lung fibroblasts by the lack of mRNA expression of *MYH11* (Figure S2B), which encodes the smooth muscle myosin heavy chain subunit 11 and we found is expressed in fibroblasts after culturing in medium containing 10% serum. Both NORML and SScL pericytes expressed the known pericyte markers angiopoietin-1 (*ANGPT1*), and there was no significant difference in the levels expressed by SScL and NORML pericytes (Figure S2C). To obtain fibroblasts, dissociated tissue cells were plated in DMEM containing 10% FBS, additional glutamine (2 mM), and penicillin/streptomycin, and were passaged and maintained in this medium at 37°C.

METHOD DETAILS

mRNA sequencing

Total RNA from 3 SScL isolates and 4 NORML isolates was sent to Novogene (https://en.novogene.com) for RNA-seq analysis. Quality control, library preparation and RNA-seq analysis were performed by Novogene as previously described.[64]

Gene level analysis

The differential expression analysis comparing "SScL versus NORML" was performed using DESeq2 R package.[65] The resulting p-values were adjusted using the Benjamini and Hochberg's approach for controlling the False Discovery Rate (FDR). FDR is the expected fraction of false positive tests among significant tests. We defined significant DE genes based on 2 criteria: **(1)** on the adjusted *p*-value (*padj*) < 0.05 and **(2)** on a log2 fold change (log2FC) with at least |0.6|. Genes with a *padj* < 0.05 and a log2FC > 0.6 were defined as significantly upregulated genes in

SScL pericytes, while genes with a *padj* < 0.05 and a log2FC < -0.6 were defined as significantly downregulated in SScL pericytes compared to NORML pericytes. A log2FC = 0.6 represents a linear increase of 1.5 fold, a criterion that has a significant biological relevance.[66]

Systems level analysis

Differentially expressed genes were entered in iPathwayGuide (Advaita Bioinformatics), an analytic tool that provides biological context for RNA-seq generated data. These genes were analyzed in the context of pathways obtained from the Kyoto Encyclopedia of Genes and Genomes (KEGG) database[67] and gene ontologies (GO) from the Gene Ontology Consortium database.[68] iPathwayGuide scores pathways using the "impact analysis" method described in detail in Nguyen et al.[69–72]

Functional enrichment of all DE genes was performed using ToppFun (ToppGene Suite), a portal for gene list enrichment analysis and candidate gene prioritization based on functional annotations and protein interactions network.[73] GO terms were then visualized using REViGO, a tool that summarizes long lists of GO terms by removing redundant ones and generates semantic similarity-based scatterplots for the remaining terms.[74]

RNA extraction and qPCR

For validation of target expression, total RNA was isolated from cells used for RNA-seq as well as independent samples using the Aurum™ Total RNA Mini kit (Bio-Rad, Hercules, CA) in conjunction with DNase treatment as per the manufacturer's specifications. Total RNA was reverse transcribed to cDNA using iScript Reverse Transcription SuperMix (Bio-Rad). Quantitative PCR analysis (qPCR) was done using a Bio-Rad CFX Connect™ instrument with ABI TaqMan Gene Expression Assays (ThermoFisher Scientific, MA). Quantification of gene expression was normalized to *B2M* as an endogenous control. The following Taqman assays were used: *ANGPT1* (Hs00375822_m1), *B2M* (Hs00187842_m1), *FIGF* (a.k.a *VEGFD*; Hs01128659_m1), *GNG4* (Hs00189551_m1), *MYH11* (Hs00224610_m1), *PTGER2* (Hs00168754_m1) and *PTGER3* (Hs00168755_m1). Relative expression was determined by the $2^{-\Delta\Delta CT}$ method.

cAMP assay and pAKT/AKT Westerns

NORML and SScL pericytes were plated at a density of 8 x 10^5 cells/well in a 6-well dish coated with 0.2% gelatin. After an overnight serum starvation, cells were stimulated with either vehicle, PGE2 at 500 nM (Cayman Chemical, catalog #363-24-6), or forskolin at 100 μM (BioVision EZSolution, catalog #26625) for 15 minutes. Lysates were prepared and analyzed using the Parameter Competitive cAMP Assay (R&D Systems, Inc. Minneapolis, MN; catalog #KGE002B) according to the manufacturer's instructions. The maximum limit of detection for this assay is 240 pmol/ml. For the pAKT/AKT Westerns, lysates were subjected to non-reducing SDS-PAGE (10% polyacrylamide) and separated proteins were transferred to nitrocellulose. After blocking in 5% BSA, membranes were probed for pAKT (Ser-473, Cell Signaling, catalog #9271), stripped with Restore™ PLUS Western Blot Stripping Buffer (Thermo Fisher Scientific), and probed for total AKT (Cell Signaling, catalog #9272). Bands were visualized using a LICOR Odyssey FC imager and were quantified using FIJI (ImageJ).

QUANTIFICATION AND STATISTICAL ANALYSIS

All continuous variables for qPCR validation and cAMP assay were expressed as the mean ± standard deviation. The statistical analyses were performed using GraphPad Prism version 9 for Windows (GraphPad Software, CA). Student's t test or Mann-Whitney test was used for qPCR data (two-group comparisons) and 2-way ANOVA followed by Tukey's multiple comparisons test were used for cAMP assay data and phospho AKT Western blot. All *p*-values < 0.05 were considered statistically significant. The statistical details of experiments can be found in the figure legends under the Results section.